Solar Photovoltaic Power Intermittency and Implications on Power Systems

Solar Photovoltaic Power Intermittency and Implications on Power Systems

Edited by

Mohammed Albadi and Abdullah Al-Badi

Cambridge
Scholars
Publishing

Solar Photovoltaic Power Intermittency and Implications
on Power Systems

Edited by Mohammed Albadi and Abdullah Al-Badi

This book first published 2021

Cambridge Scholars Publishing

Lady Stephenson Library, Newcastle upon Tyne, NE6 2PA, UK

British Library Cataloguing in Publication Data
A catalogue record for this book is available from the British Library

TABLE OF CONTENTS

PREFACE

Solar photovoltaic (PV) systems have experienced a tremendous increase in installed capacity in the past decade. The global solar PV installed capacity increased from 5.2 GW in 2005 to 627 GW by the end of 2019. This rapid growth of solar PV system deployment is expected to continue due to several factors such as PV technology improvements and cost reduction, as well as policies and regulations promoting the use of renewable energy resources. Although solar PV power is environmentally friendly and can be used to extend the life of fossil fuel reserves, it has an intermittent nature. The implications of this intermittency need to be understood by all stakeholders. In general, there are two main impacts of intermittent renewable-based generation facilities on power system operation: variability and uncertainty.

Variability of solar output can affect different operational aspects of distribution and transmission systems including power quality, losses and congestions. Intermittency of solar PV power affects the balance between supply and demand; hence the entire power system's planning and operation. For example, when the supply-demand balance is not maintained, power system frequency deviates from steady state values; consequently, system stability and reliability are jeopardized. Although it is technically possible to integrate a large number of intermittent renewable-based facilities in power systems, higher penetration levels result in more challenges to power system stability and reliability. These challenges are quantified using intermittency integration costs.

The objective of the book is to present an overview of solar PV power output intermittency and the impacts of power systems. This book contains 9 chapters. Chapter 1 covers the origin of solar irradiation variabilities and their time scales as well as different factors that affect variability such as Earth's orbital eccentricity, geometry, rotation, and axial tilt, the effect of the atmosphere and cloud cover, the effect of the solar cycle and other long-term effects. Chapter 1 also includes modeling the solar irradiation on horizontal and tilted surfaces. Chapter 2 focuses on the effect of temperature on PV systems' output power variability. The chapter includes the effect of ambient temperature variation on PV system design and system performances

and presents the PV output variability and PV cell temperature variability for a hot and dry location. In addition, the correlation between the PV output power and the PV cell temperature is also showcased and the detailed model of PV system design, system performance analysis, and variability analysis is outlined. Chapter 3 presents a case study of PV systems' output variability. The study used 15-minute average data recorded from 3 sites to study the smoothing effect of aggregating different PV systems' output on both deterministic and stochastic variabilities. The implications of deterministic variabilities were demonstrated during the annular eclipse that occurred on 21 June 2020. The smoothing effect that can reduce the stochastic variabilities, which are caused by cloud fronts, is also demonstrated. Chapter 4 focuses on the impact of dust and shading on solar PV systems' output. The chapter summarizes the research relating to the different types of dust particles that affect the efficiency of PV systems. PV system performance indices for Western Australian climatic conditions are demonstrated using experimental setups. Chapter 5 studies the impact of the integration of large-scale PV power plants on the grid stability and operation. The system steady-state stability is investigated with and without external controllers installed at the PV power plants. In addition, the chapter studies the transient stability of the power system in the presence of large-scale PV stations. Chapter 6 addresses the evaluation of the capacity credit or value of renewable energy systems, particularly photovoltaic (PV) plants in a power generation system. The chapter starts by giving an overview of the various adequacy measures used to evaluate generation system reliability and then concentrates on the evaluation of the capacity value of PV plants. Chapter 7 addresses the impacts of energy systems' output variability on transmission and distribution networks. The chapter introduces the Power Flow tool, which is used to analyze the instantaneous active and reactive power flow. The chapter includes other topics such as the integrity of multiple renewable energy resources as well as interconnection and islanding control. Chapter 8 focuses on the role of energy storage systems in reducing the negative impacts of PV systems on power systems. It includes an overview of energy storage technologies and discusses how each technology can benefit the power system to alleviate the impacts of solar PV generation. The concept of dispatchable PV-energy storage hybrid systems is also discussed. The realization of dispatchable solar PV generation can reduce the need for flexibility and reserves. A framework for dispatchable solar PV generation is proposed. The components of this framework and the tasks each should carry out are articulated. Chapter 9 presents a case study about a nearly net-zero energy building (Eco-house). The house was built on the Sultan Qaboos University (SQU) campus and

provides a high level of comfort. It has two stories, is connected to the electric grid and is equipped with a 20-kW rooftop PV system. The net energy consumed in the SQU Eco-House is 945 kWh annually which is less than 3.5% of the energy demand supplied by the electrical network. Thus, the SQU Eco-House is a nearly zero energy building.

We hope this mix of presentations will attract a large number of interested readers. The editors of this book would like to thank all the contributors for their continued support and hard work. We would like to thank the reviewers who provided valuable comments to improve the quality of this work.

We also thank the publisher for agreeing to publish this book. Finally, we would like to thank all authors for their contributions and our families for their support.

<div align="right">

Mohammed Albadi and Abdullah Al-Badi
October 2020

</div>

CHAPTER ONE

SOLAR IRRADIATION AND ITS VARIABILITY

ALAA I. IBRAHIM[1]

"*The Sun will be the fuel of the future*"
Popular Science, 1876

Abstract

Solar energy is the most prolific and accessible form of renewable energy. During the last decade, solar power has become the fastest-growing energy sector, with the worldwide solar power generation increasing by more than 30-fold, outperforming the growth rate of all other renewable energy sources combined by more than an order of magnitude. More importantly, solar energy is more equitable among countries with varying economic and development stature and has the narrowest production gap among renewable energy sources between such countries. As a perpetual source of energy, solar power is used for a wide variety of applications and can be utilized at both small and large scales. However, like all forms of natural renewable energy, solar energy has its own challenges. While new technologies and innovations are improving efficiency and reducing costs, there are variabilities and constraints that need to be understood and when possible mitigated for optimal utilization. Measured at the top of the atmosphere at Earth's average distance from the Sun, the intrinsic electromagnetic energy output of the Sun per unit area per unit time, known as the total solar irradiance, only varies minimally over long time scales of about 11 years (due to magnetic phenomena in the Sun). On the other hand, significant variabilities at shorter time scales of minutes to months are introduced by the eccentricity of Earth's orbit, Earth's rotation and axial tilt, the geometry of Earth's surface, atmospheric processes, and cloud cover.

---

[1] Department of Physics, College of Science, Sultan Qaboos University, Muscat, Oman, Email: aiibrahim@squ.edu.om.

These dynamical variabilities change by geographic location and by date and time at the same location. Here we present a comprehensive overview and analysis of the energetics of the solar irradiation and the different variabilities and constraints associated with it as observed from Earth. We start from the fundamental principles of solar radiation then address the origin and time scale of each source of variability. The solar irradiance and the integrated hourly and daily irradiation of direct Sun light are calculated for horizontal and arbitrarily tilted surfaces. Our general treatment should be useful for photovoltaic solar power purposes as well as other techniques of harnessing solar energy. We discuss approaches that can reduce the uncertainty associated with some variabilities. We conclude that despite these variabilities, the greater parts of the world receive considerable sunshine hours annually, which make solar energy a viable option. The largest regions receiving the maximum solar irradiance and least affected by its variability are those in North Africa and the Arabian Peninsula.

Keywords: Solar irradiation, irradiation variabilities, electromagnetic radiation, orbital eccentricity, cloud cover, hourly and daily solar irradiation.

1. Introduction

The term solar energy refers to the radiant electromagnetic radiation from the Sun, which can be harnessed using a variety of technologies such as photovoltaics (PV; converting solar radiation into electricity through solar panels that utilize the photoelectric effect), solar heating or solar thermal energy (collecting heat by absorbing solar radiation with or without focusing), solar architecture (utilizing the illumination and heating effects of solar radiation in architectural design), and artificial photosynthesis (utilizing solar radiation in chemical processes that mimic the natural process of photosynthesis) (van der Hoeven 2011). We will be concerned here with solar energy in the context of photovoltaics' power generation, but much of the consideration and treatment discussed is relevant and applicable to most of the aforementioned forms of solar energy harnessing.

In recent years, the utilization of solar energy has been growing steadily, thanks to advancements in photovoltaic technology that improve the efficiency and reduce the cost, as well as global and local environmental, economic, and policy reforms (Shubbak 2019, van der Hoeven 2011). Over the last decade, the worldwide generation of solar power grew from 21 TWh (Terra Watt hour) in 2009, 3% of the total renewable energy generation then, to 724 TWh in 2019, 26% of the total renewable energy generation during that year (Ritchie & Roser 2020; Looney 2020), making solar energy

the fastest growing source of renewable energy. The growth rate is also significant on short timescales. The one-year growth rate between 2018 and 2019 is 24%. Furthermore, solar energy is becoming more accessible and equitable among countries of otherwise varying levels of socioeconomic development. The share of solar power generation by non-OECD[2] countries, which are predominantly developing countries, has been rising consistently over the past decade as measured by the production gap between OECD (mainly high income, developed countries) and non-OECD shares relative to the worldwide total. This gap narrowed from 94% in 2009 to only 7% in 2019. See Table 1-1 for the trends and comparisons between solar energy, wind, and other renewable energy sources between 1990 and 2019.

Table 1-1: Renewable Energy Power Generation Over Two Decades[3]

The worldwide rate, as well as the shares of the OECD and non-OECD countries, is given. The 1990, 2009, 2019 rates show the long-term growth whereas the 2018 rates are provided to show the most recent annual growth compared with 2019.

|	1990		2009		2018		2019		2009-2019
	World (TWh)	(OECD – Non-OECD)/ World	World (TWh)	(OECD Non-OECD/World	World (TWh)	(OECD Non-OECD/World	World (TWh)	(OECD – Non-OECD)/World	Growth Rate
Solar PV	0.4	93.8%	21.0	94.0%	582.8	13.2%	724.1	6.9%	3348.1%
Wind	3.6	99.3%	276.1	64.5%	1270.2	17.4%	1429.6	17.8%	417.8%
Other Renewables	117	73.0%	339.6	43.3%	615	19.3%	651.8	19.0%	91.9%
Total	121	…	636.7	…	2468	…	2805.5	…	340.6%

We begin by reviewing how the solar radiation is produced, the components and model of the solar spectrum, and how the solar irradiance and integrated irradiation are measured. We then look at the origins, type, and time scale of the irradiation variability and how they affect the solar irradiance received on Earth. Hourly and daily rates of irradiation are obtained for horizontal and tilted surfaces at any day, time, and geographic location.

What makes solar energy special is simply the magnitude of the power received from the Sun. Among the various natural sources of energy available, solar energy delivers more power than all other natural sources combined. The power per unit area received from the Sun at the Earth's surface (global average) exceeds all other natural sources by a factor of 2600
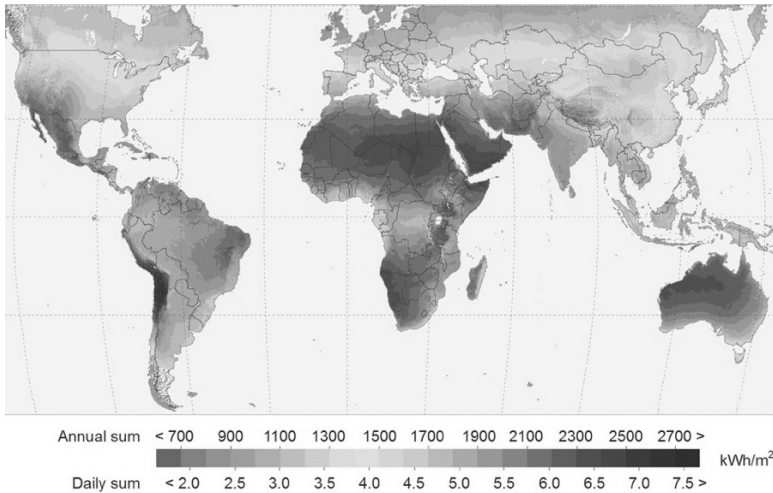
[2] Organization for Economic Co-operation and Development.
[3] Raw data obtained from (Ritchie & Roser 2020 and Looney 2020).

(Kren et al. 2017, Sellers 1965). At the top of the atmosphere this factor is
3700. Fig. 1-1a illustrates the total energy reservoirs available on Earth from
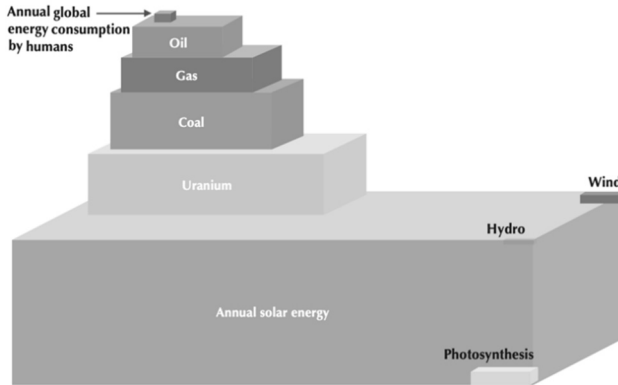
(a)

(b)

Fig. 1-1: (a) Total energy reservoir available from different sources on Earth
compared to the annual solar energy received by Earth and the annual global energy
consumption by humans. (b) World map of the global horizontal solar irradiation,
showing the long-term average of the annual and daily irradiation sums in kWh m^{-2}.
Source: IEA 2011; SolarGIS, GeoModel Solar 2013.

various sources compared to the annual solar energy received at the Earth and the human annual global energy consumption at the present time (van der Hoeven 2011).

Fig. 1-1b illustrates the global average of the daily and annual solar irradiation on a horizontal surface worldwide where the effects of geographic location and environmental and weather conditions can be inferred. Still, most inhabited regions of the world receive greater than 1300 kWh m^{-2} annually or greater than 3.5 kWh m^{-2} daily.

2. Solar Radiation

As a star, the Sun is the dominant body in the solar system, comprising 99% of its mass. Unlike Earth and other members of the solar system, the Sun has the right composition and conditions that allow for the production of abundant and steady energy over extremely long time spans (billions of years). The Sun is a dwarf main-sequence star with a mean volumetric radius of 695,700 km (nearly 110 times that of the Earth) and is situated at an average distance of 149.60×10^6 km, or 1.00 AU (astronomical unit), from Earth (Williams 2018). As a result, the Sun has an apparent angular size of 0.5° in the sky, which is similar to that of the Moon. The mass of the Sun, 1.9885×10^{30} kg, is made of 70.6% hydrogen, 27.4% helium, and 2% other gases (Williams 2018). The enormous gravity of the Sun, due to its mass, which keeps Earth and the other planets in orbit, also compresses and heats up the gasses and plasma inside the Sun. The temperature is highest at the core, reaching upwards of 10^7 K (Carroll & Ostlie 1996).

Under such conditions of extreme temperature, pressure, and density, gasses are ionized into hot and dense plasma. The collisions between the nuclei of the hydrogen atoms in the core become energetic enough to fuse them together in a nuclear fusion, which produces helium nuclei and releases electromagnetic radiations, which at this stage are high-energy photons in the X-ray and gamma-ray wavelengths, and sub-atomic particles (neutrinos and positrons). As they propagate outwards, the electromagnetic radiations are first trapped by the dense layers of the Sun's interior, undergoing millions of collisions with the dense plasma in a process known as random walk that takes up to hundreds of thousands of years and results in significant softening of the radiation to longer, less energetic wavelengths. The radiations will eventually reach the surface layer of the Sun (the photosphere), while primarily in the visible and infra-red wavelengths, with smaller components in radio, ultra-violet, X-ray, and gamma-ray wavelengths,

then arrive at Earth 8 minutes later with the spectrum we are familiar with. This spectrum, as observed at the top of the atmosphere and at Earth's surface, is shown in Fig. 1-2.
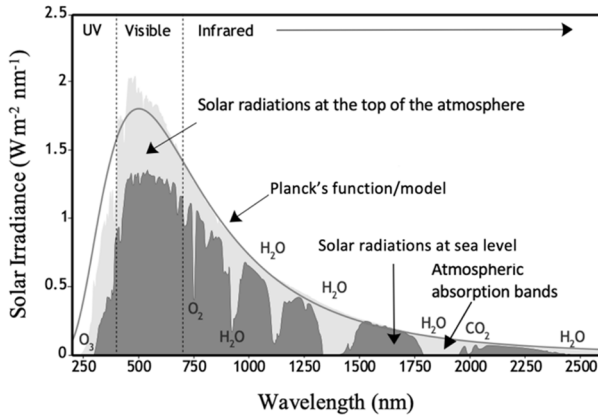

Fig. 1-2: The spectrum of direct solar radiation at the top of Earth's atmosphere (light gray) and at Earth's surface (sea level) (dark gray). The spectrum is well described by the theoretical Planck function/model (solid black line). As the radiations of different wavelengths pass through the atmosphere, some are absorbed by the atmospheric gases and molecules (e.g., water vapor H_2O and carbon dioxide CO_2), resulting in specific absorption bands. *Source: Wikimedia Commons 2013*.

About 23% of the solar radiations that arrive at the top of Earth's atmosphere are reflected back to space (by clouds, atmospheric particles/reflecting aerosols) and another 6% are reflected back to space after they reach the ground by bright ground surfaces such as sea ice and snow (Enteria and Akbarzadeh 2014). The atmosphere absorbs about 23% of the solar radiations (by clouds, water vapor, dust/absorbing aerosols, and ozone) and the remaining 48% are absorbed by Earth's surface. The total absorbed by Earth's system (surface and atmosphere) is often referred to as about 71%. The radiation absorbed by the atmosphere contributes to the diffused radiation that can also reach Earth's surface.

About 99% of the energy of solar radiation is contained in the wavelength band of the near ultraviolet, visible and near infrared regions of the solar spectrum. The makeup of the radiations that reach Earth's surface is as follows: 52%–55% is infrared above 700 nm, 42%–43% is visible light (400 nm–700 nm), and 3%–5% is ultraviolet (below 400 nm). At the top of the

atmosphere, solar radiation is 29% more intense as indicated above, with an additional 8% to the ultraviolet band (Kalogirou 2014).

The solar energy arriving at Earth is quantified by the flux of electromagnetic radiation F (energy per unit area per unit time, Joule per square meter per second; J m^{-2} s^{-1}) and is also referred to as the *solar irradiance*. The flux depends on the number of photons n received per square meter per second and the photon energy $\mathcal{E}$, which can be expressed in terms of the wavelength λ (or frequency v),

$$F = n\,\mathcal{E} = n\,h\,v = n\,h\,c\,/\,\lambda$$

where h is Planck's constant (6.626×10^{-34} J s) and c is the speed of light (2.998×10^{8} m s^{-1}).

By expressing the wavelength in μm, the energy $\mathcal{E}$ and flux F can be obtained in units of electron volt (eV) and eV m^{-2} s^{-1}, respectively,

$$\mathcal{E} = \frac{1.24}{\lambda}\,,\ F = \frac{1.24\,n}{\lambda}$$

Equivalently, this gives the power received (H) per unit area (Watt per square meter, W m^{-2}), or irradiance, at the observed wavelength. But since the solar flux varies by wavelength (as n also varies with λ), see Fig. 1-2, we need to describe the irradiance per wavelength, which gives the *spectral irradiance* (J m^{-2} s^{-1} μm^{-1}), where m^{-2} refers to the unit area and μm^{-1} refers to the wavelength. As a measured wavelength λ is normally obtained over a finite interval of width $\Delta\lambda$ (which can refer to the spectral resolution), the spectral irradiance $F(\lambda)$ (in units of W m^{-2} μm^{-1}) is given by,

$$F(\lambda) = \frac{n(\lambda)\,\mathcal{E}}{\Delta\lambda} = \frac{n(\lambda)\,h\,c}{\lambda\,\Delta\lambda}$$

The measured spectral irradiance is satisfactorily described by Planck's function (the black curve in Fig. 1-2), which describes an ideal emitter (commonly called the blackbody) and depends only on the surface temperature of the emitting body and the wavelength of the radiation as follows,

$$F(\lambda) = \frac{2hc^2}{\lambda^5}\frac{1}{e^{\frac{hc}{\lambda kT}} - 1} \quad (1)$$

where T is temperature, and k is Boltzmann's constant (1.38×10^{-23} J K^{-1}). Fitting the solar spectrum to Planck's function gives the temperature of the surface of the Sun: 5778 K (5505°C).

Integrating $F(\lambda)$ over the wavelength range of interest (e.g., the visible spectrum), gives us the total power density $H(\lambda)$ (power per unit area (in units of W m^{-2})) or irradiance

$$H(\lambda) = \int_{\lambda} F(\lambda)d\lambda \quad (2)$$

If $F(\lambda)$ is discrete such that its value is approximately constant over a wavelength interval $\Delta\lambda$, the integration can be replaced by a summation

$H(\lambda) = \sum_{\lambda} F(\lambda)\,\Delta\lambda$

Integrating $H(\lambda)$ over a given period of time, over which $F(\lambda)$ is constant, gives the solar radiant energy per unit area (Joule per square meter, J m^{-2}) during such period. This is referred to as the solar irradiation, solar exposure, solar insolation, or insolation.

While the solar energy is perceived as being carried by the photons of the electromagnetic radiation, these photons are quanta of discrete electric ($\boldsymbol{E}$) and magnetic ($\boldsymbol{B}$) fields of the radiation, described by the Poynting vector

$\boldsymbol{S} = \boldsymbol{E} \times \boldsymbol{B}/\mu,$

where μ is the permeability of the medium.

The Poynting vector illustrates the role of the direction of the incident radiation. In the above treatment a normal incidence is assumed but in reality, the angle of incidence on a fixed horizontal or tilted surface will change during the day due to the changing altitude of the Sun due to Earth's rotation and from day to day during the year due to the change in the solar declination because of Earth's orbit and axial tilt. The spectral irradiance $F(\lambda)$ from the Sun may also vary over an extended period of time. So, a general treatment that takes these effects into account is given in the next section.

3. Origin of Solar Irradiation Variabilities and their Time Scales

As a glowing spherical body of hot gas and plasma with an average surface temperature of 5778 K, the Sun is a thermal emitter whose radiative properties are well explained by thermal and quantum physics and are confirmed by observations from Earth's surface and space. The Sun's total radiation flux or power density H_{sun} (energy per unit time per unit area, $J\,s^{-1}\,m^{-2}$ or $W\,m^{-2}$) at its surface can be obtained by integrating $F(\lambda)$ over all wavelengths. From equations (1) and (2) we get

$$H_{sun} = \int_\lambda F(\lambda)\, d\lambda = \sigma\, T_{Sun}^4 = 6.32\times10^7\ W\,m^{-2} \qquad (3)$$

This is known as the Stefan-Boltzmann law, where σ is the Stefan-Boltzmann constant and T_{Sun} is the average surface temperature of the Sun. This is the power density, or irradiance, emitted by the Sun in all wavelengths of the electromagnetic spectrum, not just the visible spectrum.

The total power of the Sun (energy per unit time, $J\,s^{-1}$ or W) is obtained by account for the area of radiant surface,

$$P_{Sun} = H_{sun}\, 4\pi R_{Sun}^2 = \sigma\, T^4 = 3.84\times10^{26}\ W \qquad (4)$$

where R_{Sun} is the radius of the Sun.

The solar irradiance received at the top of Earth's atmosphere on a plane perpendicular to the Sun's rays, $H_{o\perp}$, see Fig. 1-3, can be obtained by conserving the power at the surface of the Sun and that at the surface of a sphere whose radius is equal to the Earth-Sun distance,

$$H_{Sun}\, 4\pi R_{Sun}^2 = H_{o\perp}\, 4\pi R_{Earth-Sun}^2$$

$$H_{o\perp} = H_{sun} \left(\frac{R_{Sun}}{R_{Earth-Sun}} \right)^2 \qquad (5)$$

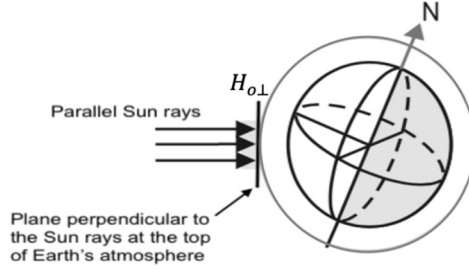where $R_{Earth-Sun}$ is the Earth-Sun distance.

Fig. 1-3: The solar irradiance $H_{o\perp}$ at the top of Earth's atmosphere on a plane perpendicular to the incident solar radiation.

The power density at the average Earth-Sun distance (1 AU) at the top of the atmosphere is called the *solar constant*,

$$H_{SC} = H_{sun} \left(\frac{R_{Sun}}{1\,AU} \right)^2 = 1366.80\ \mathrm{W\,m^{-2}}$$

H_{SC} represents the power density, or irradiance, received in all wavelengths emitted by the Sun at the top of Earth's atmosphere. It can also be referred to as the *extraterrestrial* irradiance or power density.

Integrating H_{SC} over a cross-sectional area with Earth's mean radius (6371 km), gives the total power of 1.74×10^{17} W arriving at Earth (out of the original 3.84×10^{26} W at the Sun), which is only 4.53×10^{-8} % of P_{Sun}. The actual value is even less due to Earth's curved surface.

In terms of H_{SC}, $H_{o\perp}$ of equation (5) becomes

$$H_{o\perp} = H_{SC} \left(\frac{1\,AU}{R_{Earth-Sun}} \right)^2 \tag{6}$$

3.1 Effect of Earth's Orbital Eccentricity

The first variability in $H_{o\perp}$ given in equation (5) comes from the change in $R_{Earth-Sun}$ due to Earth's elliptical orbit around the Sun (with eccentricity 0.0167086). As shown in Fig. 1-4, the distance between Earth and the Sun varies during the year from 147.10×10^6 km (0.98329 AU) during the closest approach (perihelion) on January 2-5 to 152.10×10^6 km (1.01670 AU) during the furthest approach (aphelion) on July 3-5. The average distance (149.60×10^6 km or 1.00 AU) represents the semimajor axis (Simon et al.

1994). This change in $R_{Earth-Sun}$ will cause the solar irradiance or power density to vary according to equation (5) by about 6.9% ($\pm$3.5%) between the closest and furthest approach, with the larger irradiance (1.41 kW m^{-2}) in early January and the smaller irradiance (1.32 kW m^{-2}) in early July.
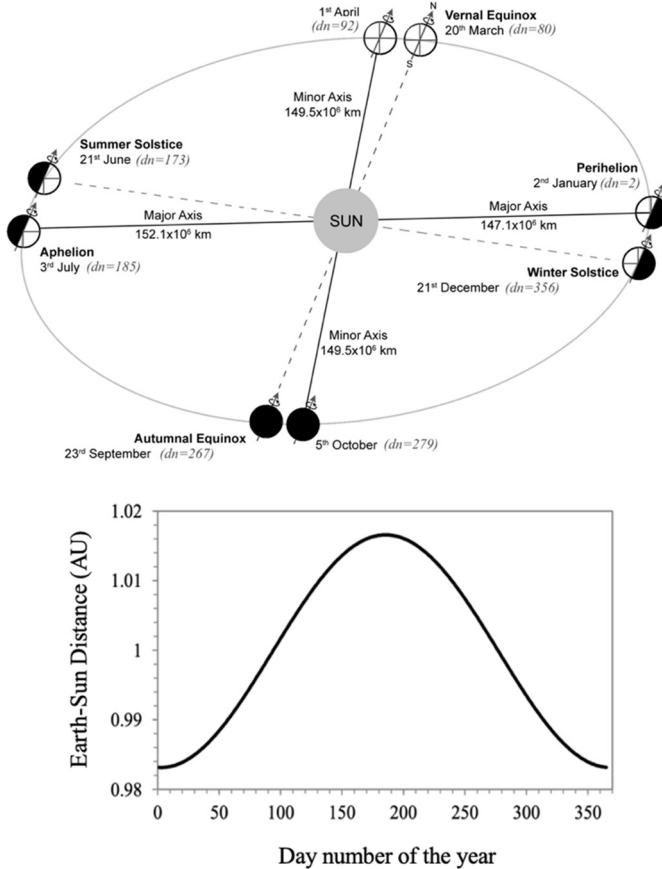

Fig. 1-4: *Top:* Earth's distance and orbit around the Sun at the different times of the year, showing the closest approach (perihelion) and the furthest approach (aphelion) as well as the Winter and Summer solstices and the Vernal (Spring) and Autumnal (Fall) equinoxes. Summer. The day number given (*dn*) is for the year 2020. *Bottom:* The variation of the distance between the Earth and the Sun by the day number.

Because the change in the distance is periodic as can be seen from Fig. 1-4 and depends only on the day number (dn, which varies from $dn = 1$ on Jan. 1st to $dn = 365$ or 366 on Dec. 31st, depending on a leap or a common year), $R_{Earth-Sun}$, and consequently the solar irradiance $H_{o\perp}$, can be expressed as a harmonic function of dn.

$$H_{o\perp}(dn) = H_{SC}\left(\frac{1\ AU}{R_{Earth-Sun}(dn)}\right)^2$$

The ratio $\left(1\ AU/\ R_{Earth-Sun}(dn)\right)^2$ is called the eccentricity correction and $R_{Earth-Sun}(dn)$ can be written as a Fourier expansion in terms of 1 AU with a number of coefficients (Kalogirou 2014, Spencer 1971, Iqbal 1983), which we write in the concise form

$$\left(\frac{1\ AU}{R_{Earth-Sun}(dn)}\right)^2 = 1\ +\ 0.033412\ \cos\left(2\pi\frac{dn-d_o}{365}\right)$$

where d_o is the day number of Earth's perihelion, or the closest approach to the Sun, which varies slightly from year to year but always occurs between January 2 and 5. For example, $d_o(2020) = 5$ (i.e., Jan. 5th), and $d_o(2021) = 2$ (i.e., Jan. 2nd).

Hence the solar irradiance at the top of the atmosphere on a given day dn is given by

$$H_{o\perp}(dn) = H_{SC}\left[1\ +\ 0.033412\ \cos\left(2\pi\frac{dn-d_o}{365}\right)\right] \qquad (7)$$

The variation of $H_{o\perp}(dn)$ with the day number through the year is shown in Fig. 1-5.
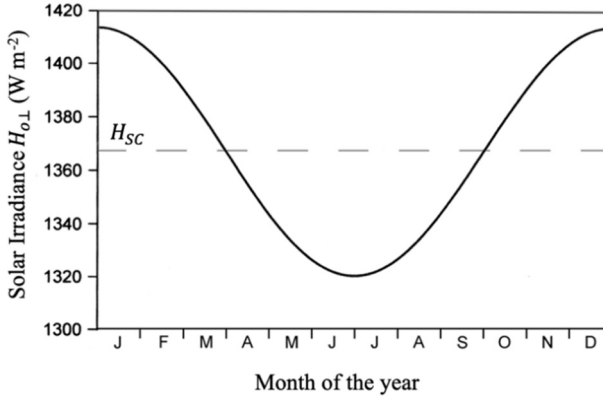
Fig. 1-5: The variability in the solar irradiance or power density $H_{o\perp}$ at the top of Earth's atmosphere over the course of one year. The dashed line represents the value of the *solar constant* H_{SC}.

3.2 The Effect of Earth's Geometry, Rotation, and Axial Tilt

While $H_{o\perp}$ on a given day is the same at all points at the top of the atmosphere whose planes are perpendicular to the incoming solar radiation, the curved surface of the Earth will dictate different angles for all horizontal surfaces other than the surface perpendicular to the line between the centers of the Earth and the Sun as illustrated in Fig. 1-6.

Let us calculate the solar irradiance at a point P' on a plane at the top of the atmosphere parallel to a horizontal surface at an arbitrary point P on Earth's surface (see Fig. 1-6). The incident parallel rays in this case make an angle θ_z with the perpendicular to the surface. The solar irradiance at P' is given by

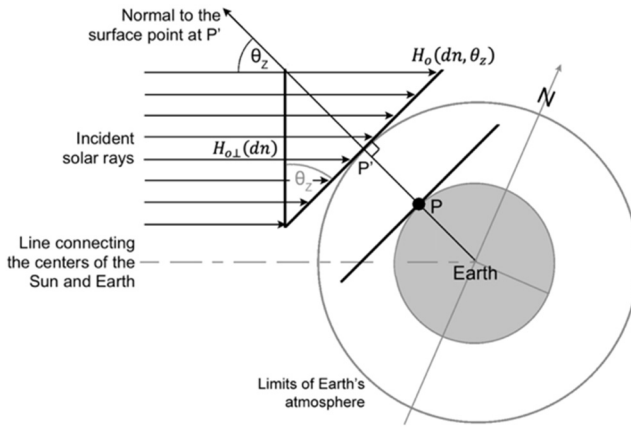$$H_o(dn, \theta_z) = H_{o\perp}(dn)\ \cos\theta_z \tag{8}$$

Fig. 1-6: A parallel beam of solar radiation incident to a plane parallel to a horizontal surface at an arbitrary point P on Earth. The incident parallel rays make an angle θ_z with the normal to the plane.

The solar irradiance will be at its maximum when $\theta_z = 0$ (normal incidence), will decrease as the θ_z gets larger (as the point P moves further north) (and equivalently further south in the southern hemisphere), and will vanish when the plane becomes parallel to the incident solar rays ($\theta_z = 90°$).

The angle θ_z is called the *solar zenith angle*, i.e., the angle between the zenith at a given location (the line perpendicular to the horizontal surface at P or P', passing by Earth's center) and the line connecting the centers of the Earth and the Sun (which defines the direction of the incident solar radiation). As shown in Fig. 1-7 and Fig. 1-8 (*Top*), the zenith angle will change: (a) during the day (from $+90°$ at sunrise to $-90°$ at sunset, passing by its minimum at the local solar noon when the Sun reaches the highest elevation in the sky) due to the apparent motion of the Sun resulting from Earth's rotation around its own axis, and (b) during the year from day to day as the Sun's elevation in the sky will change for the same geographic latitude due to Earth's axial tilt while orbiting the Sun.

Changes within the day are expressed in terms of the *solar hour angle ω*, which converts the local time and the local solar time to an angular value (with $\omega = 0°$ at solar noon, taking a positive value in the morning, and taking a negative value in the afternoon). Changes from day to day during the year are expressed in terms of the *solar declination δ*, the angle between

the plane of the equator and the line joining the centers of the Sun and the Earth, see Fig. 1-7 and Fig. 1-8. We can then write the zenith angle or $\cos \theta_z$ in terms of the solar hour angle ω, the solar declination δ, and the geographic latitude ϕ as follows,

$$\cos \theta_z = \sin \delta \sin \phi + \cos \delta \cos \phi \cos \omega \qquad (9)$$
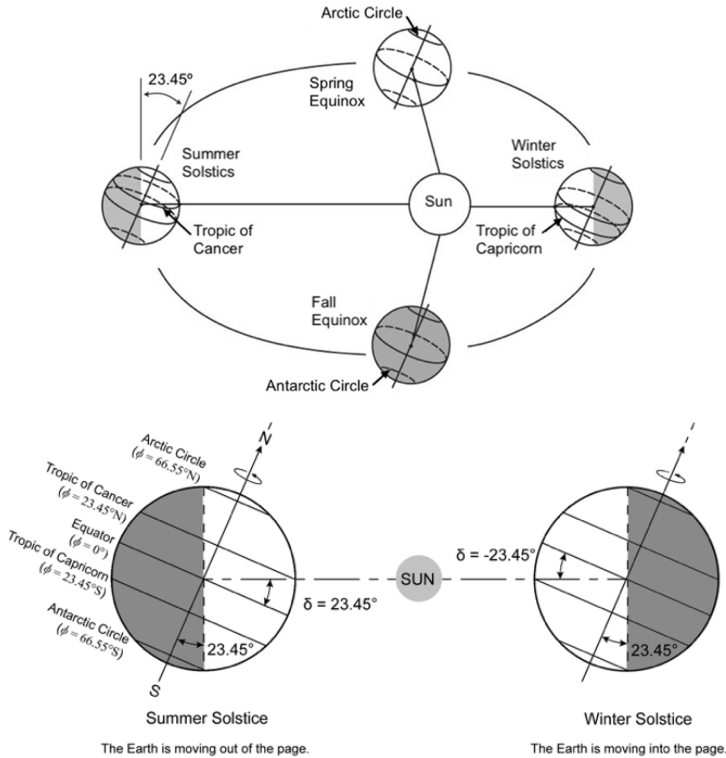

Fig. 1-7: While orbiting the Sun with an axial tilt, the elevation of the Sun in the sky changes from day to day during the year. As a result, the solar declination δ (the angle between the line connecting the centers of the Earth and the Sun and the plane of the equator) changes for each latitude.
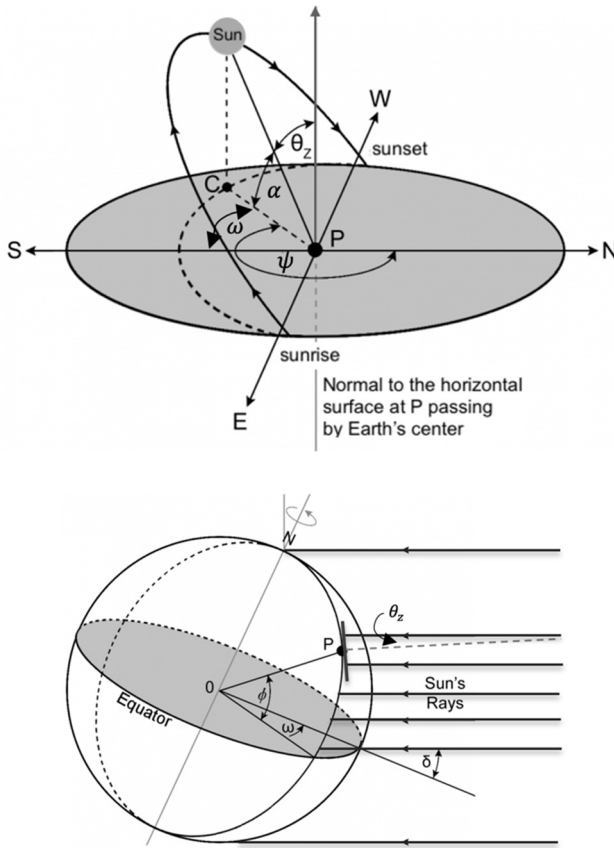
Fig. 1-8: *Top*: The path of the Sun during the day on a horizontal surface, showing the solar zenith angle θ_z, the hour angle ω, the elevation or altitude α, and the azimuth angle ψ. *Bottom:* The relation between the zenith angle θ_z at an arbitrary point P and the solar declination δ, the geographic latitude ϕ, and the hour angle ω.

The solar declination depends only on the day number dn and its variation during the year can be written as (Iqbal 1983)

$$\delta(dn) = -23.45^o \cos\left(\frac{360}{365}(dn + 10)\right)$$

The solar hour angle ω is obtained from the local solar time t_{LST} as

$$\omega(t_{LST}) = (t_{LST} - 12)\ 360^{\circ}/24hr$$

where t_{LST} is obtained in terms of the local time t_{LT} using $t_{LST} = t_{LT} + TC/60$, with $TC = 4(\phi - LSTM) + EoT$. Here, LSTM is the Local Standard Time Meridian, given by $LSTM = 15^{o}(t_{LT} - UTC)$ where UTC is the Universal Time Coordinated and EoT is the equation of time, which corrects for the eccentricity of the Earth's orbit and the Earth's axial tilt, $EoT = 9.87 \sin(2B) - 7.53 \cos(B) - 1.5 \sin(B)$, where $B = (dn - 81)\ 360/365$ and dn is the day number (Spencer 1971).

Finally, the solar irradiance on the horizontal surface can be fully obtained from the day number, latitude, and hour angle (since the solar declination is already given in terms of the day number) as

$$H_o(dn, \phi, \omega) = H_{o\perp}(dn)\ (\sin\delta \sin\phi + \cos\delta \cos\phi \cos\omega) \tag{10}$$

Integrating H_o over two hour angles ω_1 and ω_2 that correspond to a time duration of one hour, centered around ω_o, gives the hourly solar irradiation $H_{o\ Hourly}$, which we will derive in section 4 to be

$$H_{o\ Hourly}(dn, \phi, \omega_o)$$
$$= H_{o\perp}(dn)\left[\sin\delta \sin\phi + \frac{24}{\pi}\sin\frac{\pi}{24}\cos\delta \cos\phi \cos\omega_o\right] \tag{11}$$

The daily irradiation $H_{o\ Daily}$ can be obtained by integrate $H_{o\ Hourly}$ between the sunrise and sunset hour angles, which as we will derive in section 4 is given by

$$H_{o\ Daily}(dn, \phi, \omega_s)$$
$$= \frac{24}{\pi}H_{o\perp}(dn)\left[\omega_s\frac{\pi}{180}\sin\delta \sin\phi + \cos\delta \cos\phi \sin\omega_s\right] \tag{12}$$

The hour angle at sunrise and sunset $\pm\omega_s$ can be obtained by setting $\theta_z = 0$ in equation (9), which gives

$$\cos\omega_s = \frac{-\sin\delta \sin\phi}{\cos\delta \cos\phi} \quad , \quad \omega_s = \cos^{-1}(-\tan\delta\ \tan\phi) \tag{13}$$

where the hour angle of sunrise is $+\omega_s$ and that of sunset is $-\omega_s$.

The length of day, or duration of sunshine under a clear sky, is therefore $2\omega_s$, which can be converted from degrees to hours as follows (as Earth rotates by $360°$ in 24 hours)

$$Length\ of\ Day\ (hr) = 2\omega_s\left(\frac{24\ hr}{360°}\right) = \frac{2}{15}\ \omega_s$$
$$= \frac{2}{15}\ \cos^{-1}(-\tan\delta\ \tan\phi) \quad (14)$$

3.3 Effect of the Atmosphere

The propagation of solar radiation to Earth's surface through the atmosphere results in a number of effects. As discussed earlier, the atmosphere will reflect back to space about 23% and absorb another 23% while 54% will reach Earth's surface. Fig. 1-2 shows a reduction in the solar irradiance due to atmospheric absorption, scattering and reflection. A modification of the spectral distribution due to selective absorption and scattering by the atmospheric gases and particles also takes place. Furthermore, the atmosphere introduces a diffused or indirect component to the solar radiation reaching Earth's surface. These effects will clearly depend on the path of the radiation through the atmosphere. A normal incidence (shortest path) will incur the least of these effects while a shallow incidence (longer path) will incur the most. To describe this mathematically, we define the air mass (AM) as

$$AM = \frac{1}{\cos\theta_z} \quad\quad\quad (15)$$

where θ_z is the same solar zenith angle. As shown in Fig. 1-9, at the top of the atmosphere $AM = 0$ and for a normal incidence at Earth's surface $AM = 1$ ($\theta_z = 0$) and decreases for an oblique incidence ($\theta_z > 0$).
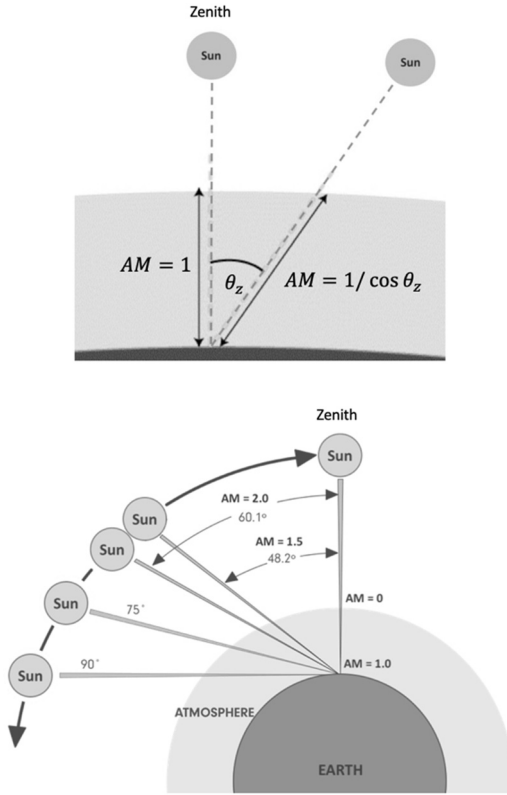
Fig. 1-9: Illustration of the Air Mass (AM) for a simplified flat atmosphere (top) and a curved atmosphere (bottom). The expression $AM = 1/\cos\theta_z$ assumes a flat atmosphere and is only approximate.

However, since the atmosphere is rather curved and not a flat layer as implied by the simplified AM expression (equation (15)), the air mass is not simply the same as the atmospheric path length, especially when the Sun is close to the horizon. For example, at sunrise and sunset θ_z is nearly 90°, which would lead to an infinite air mass while the path length is finite. An expression that takes into account the curvature of Earth and the atmosphere is given by (Kasten & Young 1989)

$$AM = \frac{1}{\cos\theta_z + 0.50572(96.07995 - \theta_z)^{-1.6364}} \qquad (16)$$

Taking this into account, the solar irradiance due to direct sun light on a horizontal plane parallel to Earth's surface is given by

$$H_s(dn, \phi, \omega, AM) = H_o(dn, \phi, \omega)\, e^{-\kappa\, AM} \qquad (17)$$

where $H_o(dn, \phi, \omega)$ is the irradiance at the top of the atmosphere given by equation (10) and κ is the atmospheric extinction coefficient due to Rayleigh scattering by gases in the atmosphere, scattering by particulate matter (aerosols), and molecular absorption.

3.4 Effect of Cloud Cover

We now consider the impact of clouds on the solar irradiance. Cloud cover poses a considerable impact on the solar irradiance at Earth's surface. Empirical models and time series analysis are used with meteorological data to estimate the average daily solar irradiation under cloudy skies and to forecast the next hour solar irradiance (Dazhi, Jirutitijaroen, & Walsh 2012; Nimnuan & Janjai 2012). The effect of the cloud cover will result in shortening the duration of sunshine (or length of day) on a given day. If S_o is the clear sky sunshine duration (i.e., corresponding to the daytime length in hours $= 2\,\omega_s/15$) and S is the reduced sunshine duration due to cloud cover, we define the cloud fraction C_f as the fraction of the daytime that the sky is obscured by clouds. C_f can be obtained from the relation

$$S = S_o(1 - C_f), \qquad or \qquad C_f = (1 - S/S_o) \qquad (18)$$

The daily solar irradiation under a cloudy sky, $H_{c\,Daily}$, can be written as

$$H_{c\,Daily}(dn, \phi, \omega_s, AM) = H_{Daily}(dn, \phi, \omega_s, AM)\left[1 - C_f(1 - T)\right] \quad (19)$$

where T is a parameter that gives the fraction of solar radiation transmitted through the clouds (Mani et al. 1967).

The cloud fraction C_f can be obtained from direct empirical measurements of the actual clear sky duration of the day S and/or meteorological data.

The variability of cloud cover during the day will impact the hourly solar irradiation in a similar fashion. To account for the different degrees of cloudiness (averaged over one hour), e.g., partially cloudy skies and passing and scattered clouds, we define the Clearness Index C_i, which is the ratio of the observed irradiance at a given time of the day to the clear-sky irradiance at the same time.